Limit on the Flux of Cosmic-Ray Magnetic Monopoles from Operation of an Eight-Loop Superconducting Detector

M. E. Huber,[a] B. Cabrera, M. A. Taber, and R. D. Gardner
Department of Physics, Stanford University, Stanford, California 94305
(Received 23 October 1989)

An eight-loop superconducting magnetic-monopole detector has been in continuous operation for 547 days, starting 4 March 1987. Its sensing area is 1.1 m^2 for double-coincident events. The data, which contain no candidate events, set an upper limit of 7.2×10^{-13} $cm^{-2}s^{-1}sr^{-1}$ (90% confidence level) on the flux of monopoles of any mass and at any velocity passing through the Earth's surface.

PACS numbers: 14.80.Hv, 85.25.Dq, 96.40.De

Grand unification theories predict that magnetic monopoles exist[1] with the Dirac magnetic charge $g=hc/4\pi e$ and a mass greater than $\sim10^{16}$ GeV/c^2. Such massive monopoles would be relics from the early Universe, would be found only in the cosmic rays, and would travel at nonrelativistic speeds. Referring to Fig. 5, stringent theoretical limits on the particle flux of monopoles are set by the existence of the galactic magnetic field (Parker bound) and by the total mass bound on the galactic dark matter.[1] However, higher flux levels are possible in monopole-plasma-oscillation theories[2] which include in a self-consistent way the interaction of the monopole plasma on the galactic field. Superconducting detectors provide the most convincing identification of a magnetically charged particle, since the response is independent of the particle's speed, mass, electric charge, and magnetic dipole moment.[3,4]

A superconducting monopole detector is, in its simplest form, a superconducting ring connected to a low-noise sensor which monitors the persistent current in the ring. A particle with magnetic charge g passing through the ring changes the flux in the ring by hc/e (the magnetic flux emanating from the monopole), which is twice the flux quantum of superconductivity, $\Phi_0=hc/2e$. After the monopole has left the region of the ring, a change in the persistent current in the ring sustains the flux change. This current change is monitored by a SQUID (superconducting quantum interference device), a low-noise amplifier with high current and flux sensitivity.

The signal current is extremely small, and induced currents resulting from external fluctuations of the ambient magnetic field can mask monopole signals. Therefore, superconducting detectors incorporate superconducting shields to attenuate these fields. However, a monopole creates $2\Phi_0$-flux vortices where it penetrates the shield, and the vortex fields couple to the detector loops. In early detectors,[3,5] this coupling was kept manageable by providing ample distance between the loops and the shield. In the current generation of detectors, the loops are not only larger but also closer to the shield to maximize the sensing areas. This design approach requires using gradiometer loops, which are less sensitive to the vortex fields.[6,7]

A number of groups, including our own,[4] have operated second-generation superconducting detectors with sensing areas of approximately 0.05 m^2 for up to 3 years without observing any convincing candidate events.[4,5] A few groups, also including our own, have built larger third-generation detectors.[4,8] We have constructed an eight-loop detector with a sensing area of 1.1 m^2 (the largest superconducting detector to date) for double-coincident events and a signal-to-noise ratio greater than 50 for a single Dirac charge (0.05-Hz bandwidth). Here, we report on the first 547 days of operation.

Referring to Fig. 1, the detector consists of eight gradiometer pickup loops located on the surface of an octagonal prism, with one loop on each face.[8,9] The pickup loops are independent, and each 16.6×521.2-cm^2 loop consists of two planar bridge-type gradiometers connected in parallel to match the inductance of the SQUID's.[7] Thus, there are four independent current paths in each panel. The conductors are NbTi ribbon, 2 mm wide and 50 μm thick, epoxied into grooves machined into a 1.6-mm-thick glass-epoxy substrate (G-10). The support structure is an assembly of 12.7-mm-thick G-10 planks. The superconducting shield is made of lead sheeting 0.8 mm thick and it surrounds the detector at a radius of 25 cm, approximately 2 cm from the sensing loops at the corners of the octagon. External to the Dewar, another shield of high-permeability sheeting with a radius of 56 cm reduces the ambient field to 10–20 mG. Figure 1(a) shows the relative locations of the shields and detectors.

A feature of this geometry is that a monopole can induce a signal in at most two loops and, for most of the cross section, no fewer than two loops. In contrast, offsets in more than two loops must be the result of electrical or mechanical disturbances and are rejected as monopole candidates. The only monopole trajectories which lead to single-loop events are those that pass through one loop and then leave through an uncovered end of the detector ($\sim10\%$ of the total cross section) and those that pass through one loop and penetrate a wire on another loop (also $\sim10\%$ of the total cross sec-

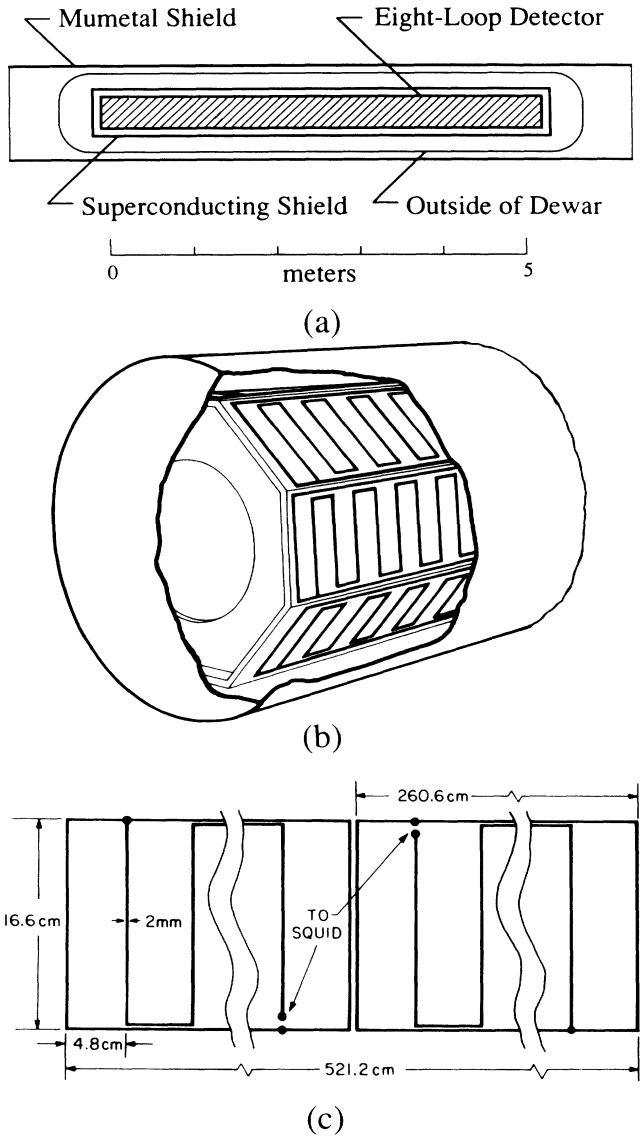

FIG. 1. (a) Schematic representation of eight-loop detector, with the superconducting shield, the Dewar, and the Mumetal shield shown. (b) Perspective view of loop structures enclosed in the superconducting shield. (c) Pickup-loop geometry.

tion). We accept only double-loop events in our calculations which determine the detector sensing area (1.5 m^2 with all panels operational).

To reduce the mutual inductance between pickup loops on adjacent panels, we alternately displace them by 2.4 cm (one-half the gradiometer cell size) along the axis of the detector. However, a residual mutual inductance remains due to an asymmetry in the gradiometer geometry. This residual coupling, as well as the effect of two open circuits in the pickup loops (to be described shortly), is included in our calculations of the expected signal magnitudes.[8,9] The signal magnitudes vary slightly depending on which section of the pickup loop is penetrated, and we have described the details of this calculation elsewhere.[8,9] The nominal current change for the passage of a Dirac charge is -170 pA at the SQUID input.

The current sensors are rf-biased SQUID's (BioTechnologies, Inc., sensors) operated at 190 MHz (Quantum Design electronics). The noise levels with the sensor loops attached are $\sim 8\times 10^{-5}\Phi_0/\mathrm{Hz}^{1/2}$ at the SQUID for frequencies greater than 0.1 Hz which corresponds to ~ 8 pA/$\mathrm{Hz}^{1/2}$. We have installed sixteen calibration coils (toroidal solenoids) at the intersection of adjacent panels, with half of them towards each end of the detector. The toroid axis is coincident with the line of intersection of the panels and each coil is located either 25 or 30 cm from each end of the panels in an alternating pattern around the circumference. This pattern is arranged so that each calibration coil couples to two pickup loops. The solenoids are constructed of No. 32 wire wound on a 20.3 cm length of No. 10-32 threaded nylon rod; an aluminum plug joins the ends of the rod to form the toroid. From measurements of calibration signals, we determine that the rms signal-to-noise ratio is greater than 50 in a 0.05-Hz bandwidth. Figure 2 shows a Dirac-size calibration signal in two loops.

We installed additional instrumentation to monitor parameters known to affect detector operation. This instrumentation includes a strain gauge attached to the exterior of the superconducting lead shield (to detect mechanical motion), a pressure transducer (to monitor the helium pressure above the liquid in the Dewar), and a power-line monitor (to detect six different fault conditions). During most of our operating period, a flux-gate magnetometer has been used to detect changes in the external field. We did not observe a significant correla-

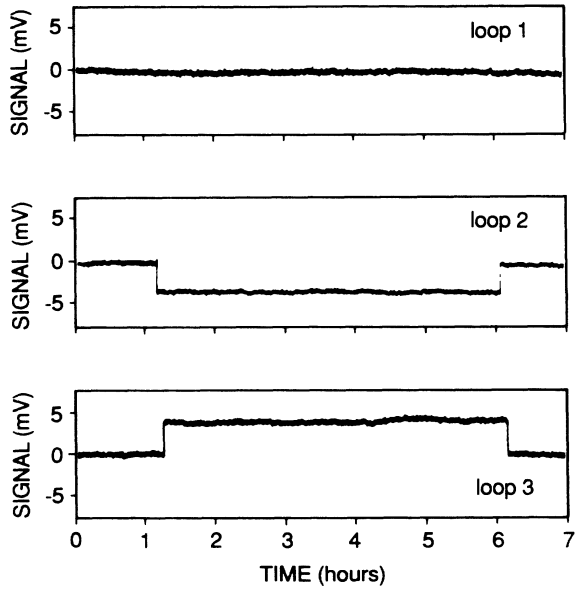

FIG. 2. Calibration signal equivalent to one Dirac charge in loops 2 and 3.

tion, though, so we have recently substituted a wideband rf voltmeter to detect changes in the local rf environment which can cause offsets in SQUID's. An ultrasonic motion detector monitors laboratory activity. When we perform activities known to disturb the detector stability, we set a "veto" switch to prevent generating large numbers of useless computer event files and to aid in calculating our live time. A closed-cycle helium liquefier connected to the Dewar eliminates helium transfers and maintains a constant liquid-helium level, so the operation can be extremely stable. Gas-cooled radiation shields eliminate the need for liquid nitrogen. A feedback circuit regulates the pressure (and thus the temperature) of the liquid helium by proportionally controlling a heater at the Joule-Thompson valve in the liquefier.

Two systems collect the data: a pair of analog strip-chart recorders and a digital computer. The strip-chart recorders record data in a 0.1-Hz bandwidth from the eight SQUID's, the pressure transducer, and the flux-gate magnetometer (most recently, the rf voltmeter). A 12-bit analog-to-digital converter collects data from the eight SQUID's, strain gauge, and magnetometer or voltmeter at a 10-Hz bandwidth (20 samples per second per channel) and digitally filters that data for long-term storage to a 0.05-Hz bandwidth (1 sample per 10 s per channel). The computer also samples data from the digital lines, the pressure transducer, and helium level at the slow rate only. The computer stores the 10-Hz data on disk whenever an offset is detected in the filtered data, unless the veto is set. Once every 2 weeks, a program searches the filtered data for offsets greater than a threshold of $\sim 0.3\Phi_0$, while ignoring slow changes and brief excursions from the base line. This operation also determines live time by discarding periods of noisy data and determines the magnitudes of any observed events.

We have characterized the detector response with a Monte Carlo simulation of random monopole trajectories, in the approximation that there is no coupling between panels and that all SQUID's are identical (Fig. 3). The method has been described in conjunction with our earlier three-loop experiment[10] and was modified for this detector geometry.[11] The signal spread of $\sim 15\%$ is caused by the random location of supercurrent vortices which appear in the shield accompanying each monopole trajectory. In reality, the detector pickup loops are not completely independent, as a result of the residual mutual inductance between adjacent panels ($\sim 10\%$ of the self-inductances[8,9]). This effect is observed primarily during calibration, when currents of the same order are induced in adjacent panels. However, when flux is applied to two nonadjacent panels, the coupling does not significantly affect the signal size. Upon cooling the detector, the conducting NbTi ribbon cracked and opened two pickup-loop circuits, causing those loop sections to be unresponsive to flux changes. We modified the trajectory-simulation program to discard all trajectories passing through those panels, and found that the active sensing area is reduced to 1.3 m^2. The overall uncertainty in the detector response to a particular monopole trajectory is dominated by the $\sim 15\%$ spread resulting from the supercurrent vortices and increases to $\sim 20\%$ when we include the uncertainties in the detector geometry.

Between 4 March 1987 and 1 September 1988, we obtained 6482.4 h of active sensing time. This active time corresponded to only 50% of the total time due to a five-month period of building, remodeling, and to problems with the liquid-helium refrigerator. During the active operation, we observed 43 single-channel offsets which did not correlate with disturbances in the anticoincidence data (Fig. 4). This number corresponds to an accidental two-loop coincidence rate in a 10-s window of one per ~ 800 yr. The incidence of double-coincident offsets is much larger than this estimate. There are four in this period of operation, but with magnitudes inconsistent with a Dirac charge and occurring only in adjacent panels. For true monopole events, we would expect to observe adjacent-panel events in 15.2% of all events, so that the probability of observing four adjacent-panel events without observing any other coincident events is $(0.152)^4 \approx 0.0005$. Instead, we believe that these events are due to mutual rf interference between SQUID's, coupled through adjacent pickup coils. All four events were observed in the first 221 days of operation, and none

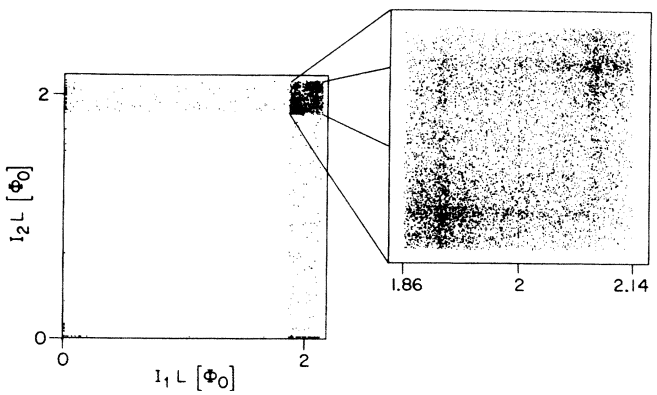

FIG. 3. Calculated response of detector to uniform flux of monopoles.

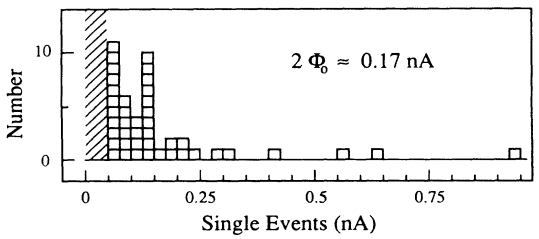

FIG. 4. Distribution of unexplained single-channel offset events above ~ 50-pA threshold (the numbers from SQUID's 1–8 were 7, 4, 5, 10, 9, 2, 3, 3 for 43 total).

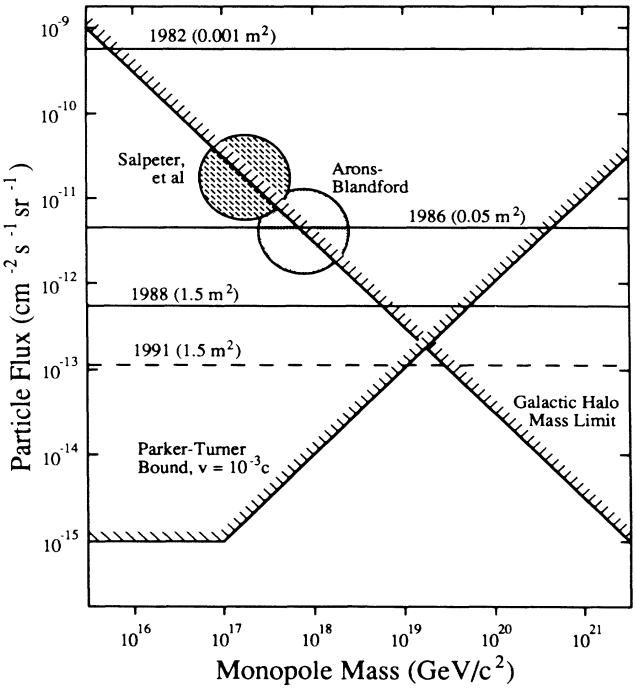

FIG. 5. Comparison of experimental and theoretical limits on magnetic-monopole flux in cosmic rays. The dotted line shows the flux limit which is attainable after two additional years of operation.

have occurred since we carefully adjusted the rf excitation frequency for each SQUID to avoid mutual resonances. Nonetheless, we have discarded the area contributed by adjacent-panel events, reducing the sensing area to 1.1 m^2.

In conclusion, these data set an upper limit of 7.2×10^{-13} $cm^{-2}s^{-1}sr^{-1}$ at 90% confidence level ($2.3/\int dA\, d\Omega\, dt$) on any uniform flux of magnetic monopoles passing through the Earth's surface at any velocity (Fig. 5). This limit is a factor of 2000 below the flux suggested by the single-candidate event seen with the prototype detector.[3] Based on this large factor and based on the noncoincident nature of the prototype detector, we conclude that the entire data set from the prototype detector which contains the single event should be discarded. In addition, this new and lower flux limit is below the level suggested by the monopole-plasma-oscillation models,[2] largely ruling out these models. The new limit is also within a factor of ~5 above the peak created by the crossover in the mass-dependent Parker bound and galactic dark-matter bound at around the Planck mass.

This work has been funded by Department of Energy Contract No. DE-AT03-82ER40-076.

---

[a]Present address: National Institute of Standards and Technology, 325 Broadway, Boulder, CO 80303.

[1]For a recent review of theory, see J. Preskill, Ann. Rev. Nucl. Part. Sci. **34**, 461 (1984).

[2]D. Chernoff, S. L. Shapiro, and I. Wasserman, Astrophys. J. **304**, 799–820 (1986); J. Arons and R. D. Blandford, Phys. Rev. Lett. **50**, 544 (1983).

[3]B. Cabrera, Phys.Rev. Lett. **48**, 1378 (1982), and references therein.

[4]For a recent review of experiments, see D. E. Groom, Phys. Rep. **140**, 323 (1986).

[5]B. Cabrera, M. Taber, R. Gardner, and J. Bourg, Phys. Rev. Lett. **51**, 1933 (1983).

[6]J. Incandela *et al.*, Phys. Rev. D **34**, 2637 (1986); S. Bermon, IEEE Trans. Mag. **23**, 1134 (1987).

[7]S. Somalwar *et al.*, Nucl. Instrum. Methods. Phys. Res., Sect. A **226**, 341 (1984).

[8]M. E. Huber *et al.*, IEEE Trans. Mag. **25**, 1208 (1989).

[9]M. E. Huber, Ph.D. thesis, Stanford University, 1988; M. E. Huber *et al.*, Stanford Low Temperature Group Report No. BC76-88 (to be published).

[10]B. Cabrera, R. Gardner, and R. King, Phys. Rev. D **31**, 2199 (1985).

[11]R. D. Gardner, Ph.D. thesis, Stanford University, 1988; R. D. Gardner *et al.*, Stanford Low Temperature Group Report No. BC61-88 (to be published).

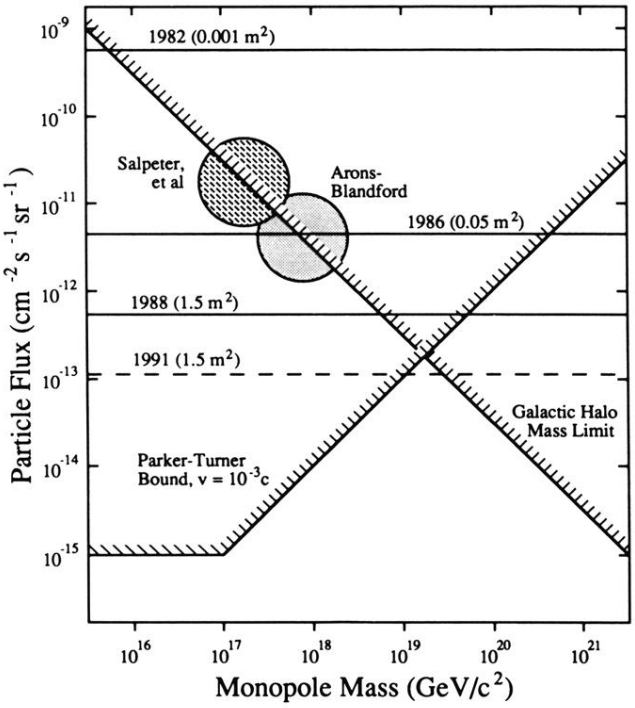

FIG. 5. Comparison of experimental and theoretical limits on magnetic-monopole flux in cosmic rays. The dotted line shows the flux limit which is attainable after two additional years of operation.